JOURNAL OF MATERIALS SCIENCE 26 (1991) 3565–3574

Development of solidification microstructures in a fibre reinforced alloy

Q. F. LI, D. G. McCARTNEY
Department of Materials Science and Engineering, University of Liverpool, PO Box 147, Liverpool L69 3BX, UK

A. M. WALKER
ICI Advanced Materials, PO Box 11, The Heath, Runcorn, Cheshire WA7 4QF, UK

The solidification behaviour of a fibre reinforced Al–6 wt% Cu alloy, containing 30 vol% of 3 μm diameter, semi-continuous, aligned alumina fibres has been studied. Results are presented to show the influence of fibres on the microstructural development of and microsegregation in the matrix during freezing. The effect of total solidification time, θ_t, on solidification behaviour was examined for $1 < \theta_t < 520$ s. By using interrupted solidification experiments microstructural development was studied in detail. It was found that α-Al begins to grow within interfibre regions, and grows towards the Al_2O_3 fibres, avoiding them where possible. Consequently fibres are located in the last regions to solidify. When $\theta_t > 10$ s the final microstructure is non-dendritic, and $CuAl_2$ is located predominantly at the fibre–matrix interface. When $\theta_t \simeq 1$ s it was observed that the final microstructure is dendritic with a periodic segregation pattern, and the $CuAl_2$ is more dispersed. The matrix composition becomes more uniform, and the minimum matrix composition rises as θ_t increases. The growth and microsegregation are analysed and discussed using simple semi-analytical models. The implications are that fibres significantly influence solidification behaviour if $\lambda_f/\lambda_s < 1$, where λ_f is the average interfibre spacing and λ_s the secondary dendrite arm spacing which would develop in the unreinforced alloy.

1. Introduction

As a result of extensive studies, the solidification behaviour of alloys is now reasonably well understood [1]. Empirical relationships have been developed [1–3] to relate microstructural features, such as primary and secondary dendrite arm spacings, to the solidification conditions, alloy constitution, phase diagram parameters, and material constants. It is, for example, generally accepted that the secondary dendrite arm spacing in an alloy, λ_s, is proportional to $(t_f)^n$ where t_f is the local freezing time and $n \simeq 0.35$ [4]. Mathematical models of dendritic growth, both columnar [5, 6] and equiaxed [7, 8] have been published by a number of authors, and the modelling of microsegregation during freezing has attracted particular attention as described by Kirkwood [9]. The techniques of (a) interrupted solidification during continuous cooling [10] (the sample being virtually isothermal at all times) and (b) quenched unidirectional solidification [4, 11, 12] (the sample being in a steep temperature gradient) have both proved particularly valuable in providing an understanding of dendritic growth, microstructural evolution and development of microsegregation in numerous alloy systems.

It is now possible to manufacture metal matrix composites in which ceramic fibres or particulate are incorporated into a metallic alloy matrix. The process of squeeze or pressure infiltration in which molten metal – most commonly an aluminium alloy – is forced into a ceramic fibre preform and then allowed to solidify has become a particularly well developed manufacturing route [13, 14]. Despite its technological importance, however, surprisingly few studies have been reported on the influence of ceramic fibres on solidification behaviour. In fact only Mortensen and co-workers [15–18] appear to have carried out systematic experimental studies combined with theoretical modelling.

Mortensen *et al.* [18] used quenched unidirectional solidification to study the freezing behaviour of an Al–4.5 wt% Cu alloy containing 140 μm diameter aligned SiC fibres. They found that in small interfibre spaces, of the order of 20 to 60 μm across, microstructural development and microsegregation were very different from that observed in the monolithic alloy for freezing times in excess of about 80 s. In the same alloy, reinforced with 20 μm diameter aligned Al_2O_3 fibres, Mortensen *et al.* [16] observed that, for a particular freezing time, microstructure and microsegregation were significantly modified if the average interfibre spacing was less than the secondary dendrite arm spacing that would have formed in the monolithic alloy. Recently Sekhar and Trivedi [19] have reported work on the interaction between fibres–narrow chan-

0022–2461/91 $03.00 + .12

nels, and solidification fronts in a transparent analogue system. This study provides clear evidence for the strong interactive effects that can occur.

The main purpose of this paper is to present results on the solidification behaviour of an Al–6.0 wt % Cu alloy containing aligned alumina fibres of 3 μm in diameter. This study differs from those of Mortensen and co-workers [15–18] in several respects, the principal one being that very much smaller diameter fibres were employed; in this case 3 μm as opposed to 20 and 140 μm, respectively. The significance of this, in terms of average interfibre spacing, is shown in Fig. 1 in which average interfibre spacing is plotted against fibre volume fraction, FV, for the three relevant fibre diameters (assuming a hexagonal array of fibres). Clearly, very small interfibre spaces of around 6 μm occur with 3 μm fibres even at fibre fractions as low as 0.3, thus low fractions of 3 μm diameter fibres are expected to strongly influence solidification in this alloy even at freezing times as short as 10 s.

The main objective, therefore, of this work was to carry out controlled cooling and interrupted solidification experiments which would provide detailed information on the following: (a) the influence of total freezing time on microstructure–microsegregation, and (b) the microstructural evolution of the growing solid aluminium phase and its interaction with the alumina fibres. These experiments were performed on squeeze infiltrated composites which were subsequently remelted and then resolidified. This ensured that variables in the squeeze infiltration process such as ceramic preform temperature, melt superheat, and melt infiltration did not affect observations on solid phase nucleation and growth.

2. Experimental procedure

2.1. Composite fabrication

The fibre reinforced metal matrix composites used in this study were initially prepared by squeeze infiltration of the matrix alloy into a binder-free ceramic preform. The matrix alloy was of composition Al–6.0 wt % Cu and was prepared from super purity aluminium (99.995 wt % Al) and high purity copper (99.9% Cu). The fibres were standard density Safimax fibres manufactured by ICI Advanced Materials, Runcorn, UK. Safimax is a semi-continuous, aligned, alumina fibre, 3 μm in diameter, with a microstructure very similar to that of Saffil [20, 21]. Fibre preforms were prepared by compressing the appropriate weight of fibres into a cylindrical steel mould 15 mm in diameter and 60 mm long. Each pre-heated mould and preform were then placed in the die of a conventional squeeze casting rig similar to that described by Clyne and Mason [13], and the molten metal was infiltrated into the preform at a pressure of approximately 7 MPa. The fibre preforms used were such as to give a fibre volume fraction of approximately 0.3 in all samples. After removal from the squeeze casting die the composite bars were carefully machined from the metal in which they were encapsulated. These bars were then cut into shorter lengths to provide samples for remelting which were 15 mm in diameter and 12 mm in height. A small hole 2 mm in diameter was drilled along the central axis of each short cylindrical sample, to a depth of approximately 7.5 mm. This was used to accommodate a thermocouple during the experiments described in the next section.

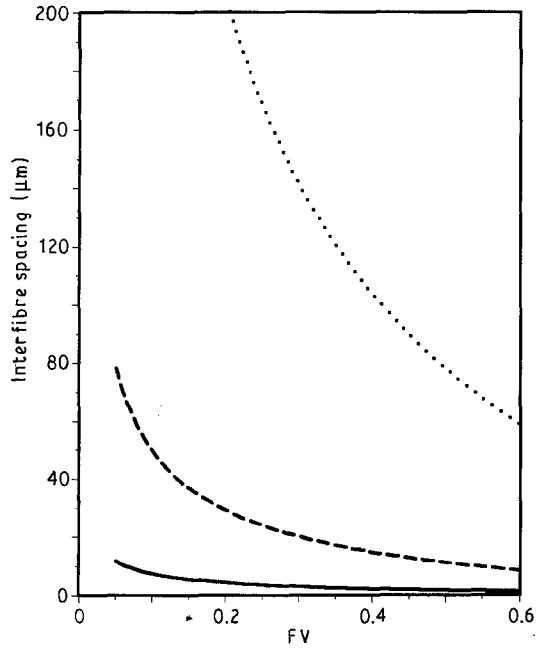

Figure 1 Plot of interfibre spacing versus fibre volume fraction, FV, for fibre diameters 3 μm (——), 20 μm (– – –) and 140 μm (·····).

2.2. Controlled solidification experiments

Composite bars were remelted and resolidified under controlled conditions using the furnace arrangement shown in Fig. 2. In this furnace samples were remelted, cooled, and then rapidly quenched into a water bath from various temperatures within the freezing range. The furnace shown in Fig. 2 consisted of four main parts: (i) an outer alumina furnace tube, (ii) a quench-tank containing water, (iii) a graphite cylinder with three 17 mm diameter holes parallel to the axis and (iv) a central steel rod, 2 mm in diameter, attached to a segmented plate beneath the graphite cylinder.

Composite samples were placed as shown and temperatures were measured using chromel–alumel thermocouples made from 0.2 mm diameter wire. Samples were heated to 720 °C, allowed to equilibrate for a few minutes prior to being cooled at a rate of approximately 0.2 $K\,s^{-1}$ in the fully liquid state. Temperature against time traces were recorded using a chart recorder, and 20 mV of the thermocouple output was backed-off to improve the resolution of the temperature measurements. Temperature resolution was thus approximately ± 0.5 K. At an appropriate temperature, within the freezing range, the rod attached to the segment plate was rotated and a sample fell from the graphite cylinder and was quenched in water. By rotating the segment plate different amounts up to three samples could be quenched in a single experimental run either at very similar temperatures or over a range of temperatures. In this way it was possible to produce a series of composite samples which were solidified under the same cooling conditions but

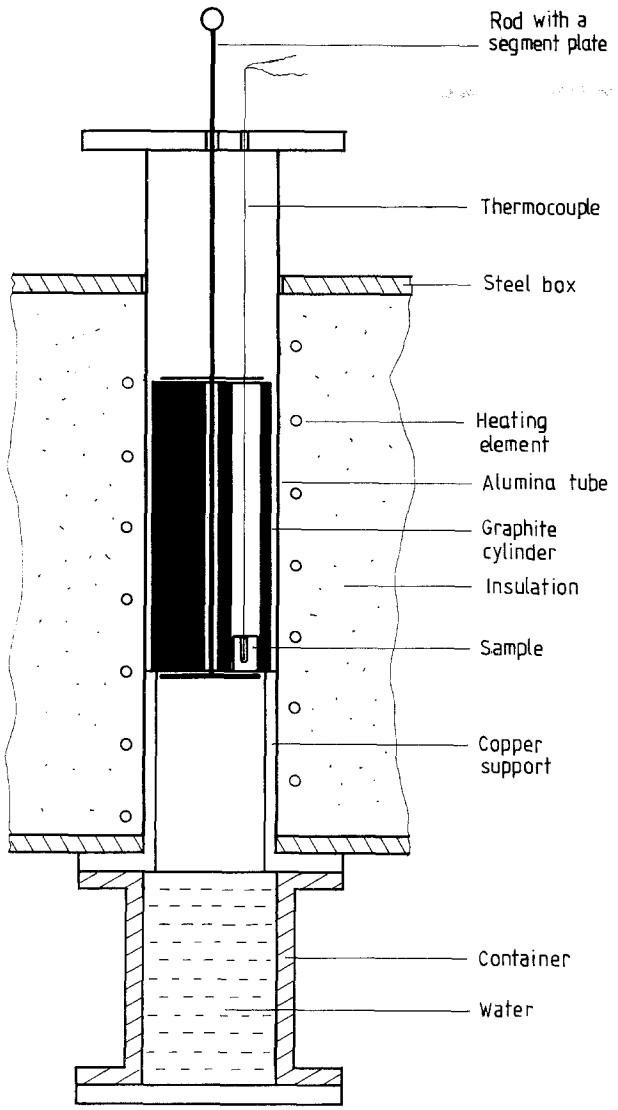

Figure 2 Schematic illustration of the furnace arrangement used for interrupted solidification experiments.

which were quenched after different local solidification times, t_f. In Table I the specimens which were produced are listed. The cooling conditions of all these samples were such that the time to total freezing would have been $\simeq 520$ s.

It should be noted that these composite samples were not melted in a crucible. This was because samples retained their shape up to the 720 °C holding temperature employed, and thus very rapid quenching was achieved due to the good thermal contact between sample and quenching medium.

In order to produce a series of specimens cooled under different conditions i.e. with different total solidification times, θ_t, composite samples of the same dimensions as used in the apparatus of Fig. 2 were subjected to furnace cooling, air cooling (with different amounts of ceramic fibre insulation) and direct water quenching; all from 720 °C. Table II summarizes the experimental data for these specimens. It should be noted that sample 7 also formed part of the series of samples listed in Table I. It was furnace cooled in the apparatus shown in Fig. 2 to just below the eutectic temperature of 548 °C and then water quenched, thus in sample 7, $\theta_t = t_f = 520$ s.

TABLE I Solidification parameters of the interrupted solidification samples

Sample	Temperature at quenching (°C)	Local solidification time, t_f (s)
1	641	18
2	641	30
3	634	90
4	625	160
5	612	220
6	583	310
7	543	520

TABLE II Solidification parameters of controlled cooling rate samples

Sample	Total solidification time, θ_t (s)
7	520
8	286
9	186
10	110
11	$\simeq 1$

Thermocouples were used to measure θ_t in samples 7 to 10. As sample 11 was prepared by water quenching a direct thermocouple measurement was not possible. Instead a non-reinforced alloy of composition Al–4.5 wt % Cu was quenched identically and its secondary dendrite arm spacing carefully measured. Using data given in reference [16] θ_t was estimated for this alloy, and the value for the composite assumed to be the same, therefore, the value of 1 s for sample 11 is an approximate one.

2.3. Metallography and measurements of microsegregation

Both fully solidified and interrupted solidification samples were sectioned parallel and perpendicular to the fibre direction for metallographic examination. Grinding and polishing was very carefully carried out in order to maintain coplanarity of hard fibres and relatively soft matrix. Final polishing was performed on a soft billiard-type cloth using a colloidal silica suspension. A colour etching technique which has been described previously in the literature [16, 18] was used to reveal matrix microsegregation in optical metallographic samples. The small interfibre spacings occurring in these samples meant that it was often difficult to obtain a uniform and consistent etching response from the $KMnO_4$–$NaOH$–H_2O mixture employed. It was found to be beneficial to clean the surface in orthophosphoric acid for a few seconds followed by washing in distilled water immediately prior to etching.

Fully quantitative matrix composition measurements were performed using a Jeol JXA-50A electron probe microanalyser fitted with a Link AN 10000 energy dispersive analysis system. Suitable areas for microanalysis were located using the colour etch and marked with microhardness indentations. The etch

was then lightly polished away, without removing the microhardness indentations, and the same area was located for microanalysis measurements. The composites were sufficiently conductive to allow analyses to be performed on uncoated samples. The operating conditions used for electron probe microanalysis (EPMA) were as follows

accelerating voltage 20 kV
beam current 2.4×10^{-8} A
X-ray take-off angle 35°
standard Al–2.46 wt % Cu (homogenized)
(composition determined by atomic absorption spectrophotometry)
characteristic lines AlK_α; CuK_α
counting time 100 s real time with a dead time $\simeq 30\%$.

Copper concentrations were determined by point analyses along pre-determined lines in the matrix. The resolution limit of the electron microprobe is around 3 μm in aluminium and so measurements were not taken from areas of the matrix where the interfibre spacing fell below 5 μm.

3. Results and discussion

3.1. Influence of total solidification time, θ_t

Five different values of θ_t were used as listed in Table II. Micrographs of transverse and longitudinal sections from samples 7, 10 and 11 are shown in Figs 3, 4 and 5, respectively. Fig. 3 shows clearly that for a θ_t value of 520 s the final microstructure was non-dendritic and that there is virtually no evidence for variations in copper concentration within the matrix. A small amount of an intermetallic phase, $CuAl_2$, formed and is seen to be located predominantly at the fibre–matrix interface. It is also apparent that the fibres did not form a regular array within the matrix. There is in fact evidence for clustering and chaining of fibres in Fig. 3a and the $CuAl_2$ has formed in such a way as to link together neighbouring fibres. The solid appears to have avoided the alumina fibres as it has grown, and there is no evidence for secondary dendrite arms in either Fig. 3a or b. (λ_s in the unreinforced alloy has been measured to be $\simeq 65$ μm for this value of θ_t.) The micrographs of Fig. 4 reveal that some matrix microsegregation occurred for a θ_t value of 110 s, but that the final microstructure remained non-dendritic. As before the $CuAl_2$ was concentrated at the fibre–matrix interface and clustering of fibres occurred giving rise to fibre free regions which are seen to be somewhat larger than the average interfibre spacing of 5.5 μm (calculated assuming a random fibre distribution with a fibre fraction 0.3 [22]). The amount of microsegregation observed in samples 8 and 9 was less than in sample 10 and so for this reason micrographs of these samples are not presented. The microstructures were also broadly similar to that shown in Fig. 4.

In Fig. 5, the micrographs from sample 11 show a quite different solidification structure and microsegregation pattern as compared with samples 7 to 10. In this instance there is clear evidence for significant variations in copper concentration within the aluminium matrix, and Fig. 5b shows a periodic compositional variation characteristic of a cast structure with secondary dendrite arms. It is also clear in Fig. 5b that the $CuAl_2$ phase was entrained within the α-Al matrix as thin channels as well as being located at the fibre–matrix interface. Sample 11 had a θ_t value of 1 s, and it has been found that the same freezing conditions gave a secondary dendrite arm spacing of approximately 6 μm in an unreinforced alloy of the same composition, thus in this case λ_s was similar to the average interfibre spacing and somewhat smaller than the diameter of the local, fibre-free regions seen in Fig. 5a.

Suitable areas for EPMA were located in samples 7 to 10 in order to confirm the optical metallographic results. Sample 11 was not analysed in this way because of the relatively small spatial scale of compositional variations. As can be seen from Fig. 5b the periodicity of segregation is around 5 μm which is only marginally greater than the resolution of EPMA. Hence meaningful composition profiles would not have been obtained with this technique.

Fig. 6a to d shows the regions (on sections perpendicular to the fibre direction) which were analysed from samples 7 to 10, respectively. The etched layers shown on Fig. 6a to d were removed prior to analysis as discussed in Section 2.3. The measured concentrations along the lines shown in Fig. 6a to d are listed in Table III. These quantitative analyses provide firm support for the interpretation of the etched microstructures (shown in Figs 3 and 4) as well as providing additional information on the samples 8 and 9 with θ_t values of 286 and 186 s, respectively. It is apparent that in sample 7 there was very little compositional variation within the matrix. In the relatively large interstice examined the minimum copper content was 4.6 wt % and the amount in solution rose to 5.4 wt % in the vicinity of fibres. This value is close to the limit of solid solubility of Cu in Al at the eutectic temperature. It is also to be expected that smaller interstices than the one examined would be of more uniform composition. It can be seen from Table III that the minimum copper concentration decreased with decreasing θ_t, but that even for $\theta_t = 110$ s the minimum copper content was well above that expected in an unreinforced alloy. The absence of measured compositions as high as 5.4 wt % Cu in samples 8 to 10 can readily be explained as follows. Regions of high copper content are only deposited from the liquid in the latter stages of freezing (close to the eutectic temperature). In sample 7 the slow cooling rate allowed appreciable solid-state diffusion of Cu into the matrix leading to homogenization, as will be discussed in detail in Section 4. In samples 8 to 10 the shorter freezing times did not allow such extensive solid-state diffusion and thus the regions of high Cu content are expected to be confined to within 1 to 2 μm of the fibre–matrix interface regions. EPMA of these areas was not carried out because the resolution limit of the technique is $\simeq 3$ μm due to beam spreading within the sample, thus in samples 8 to 10 measured copper levels as high as 5 wt % were not expected, as is indeed the case.

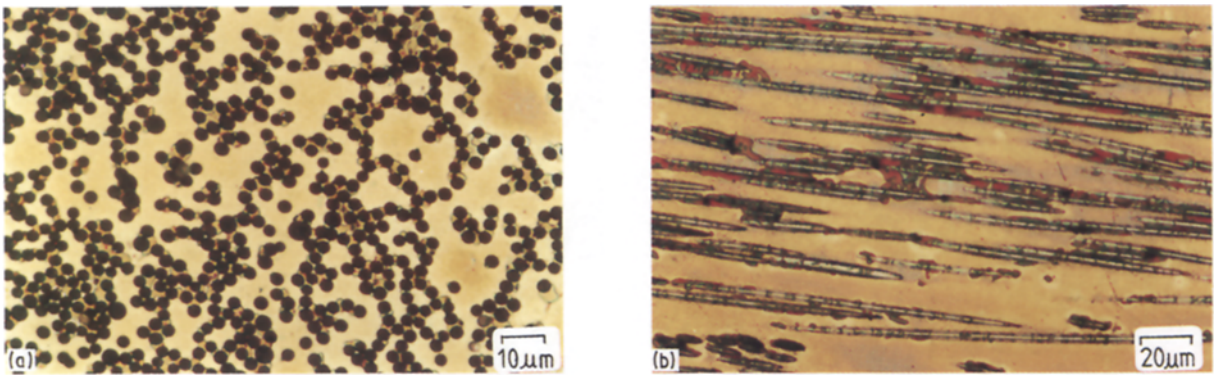

Figure 3 Optical micrographs of etched sections taken from sample 7, (a) is transverse and (b) parallel to the fibre direction.

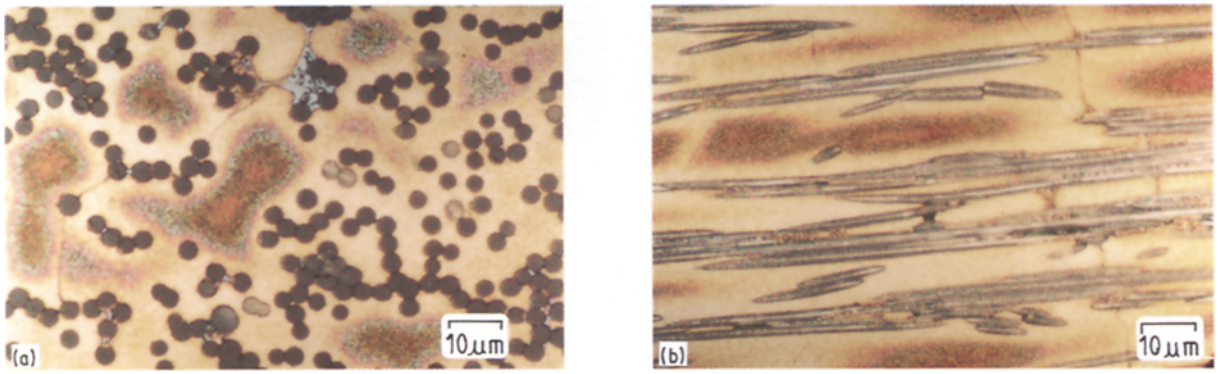

Figure 4 Optical micrographs of etched sections taken from sample 10, (a) is transverse and (b) parallel to the fibre direction.

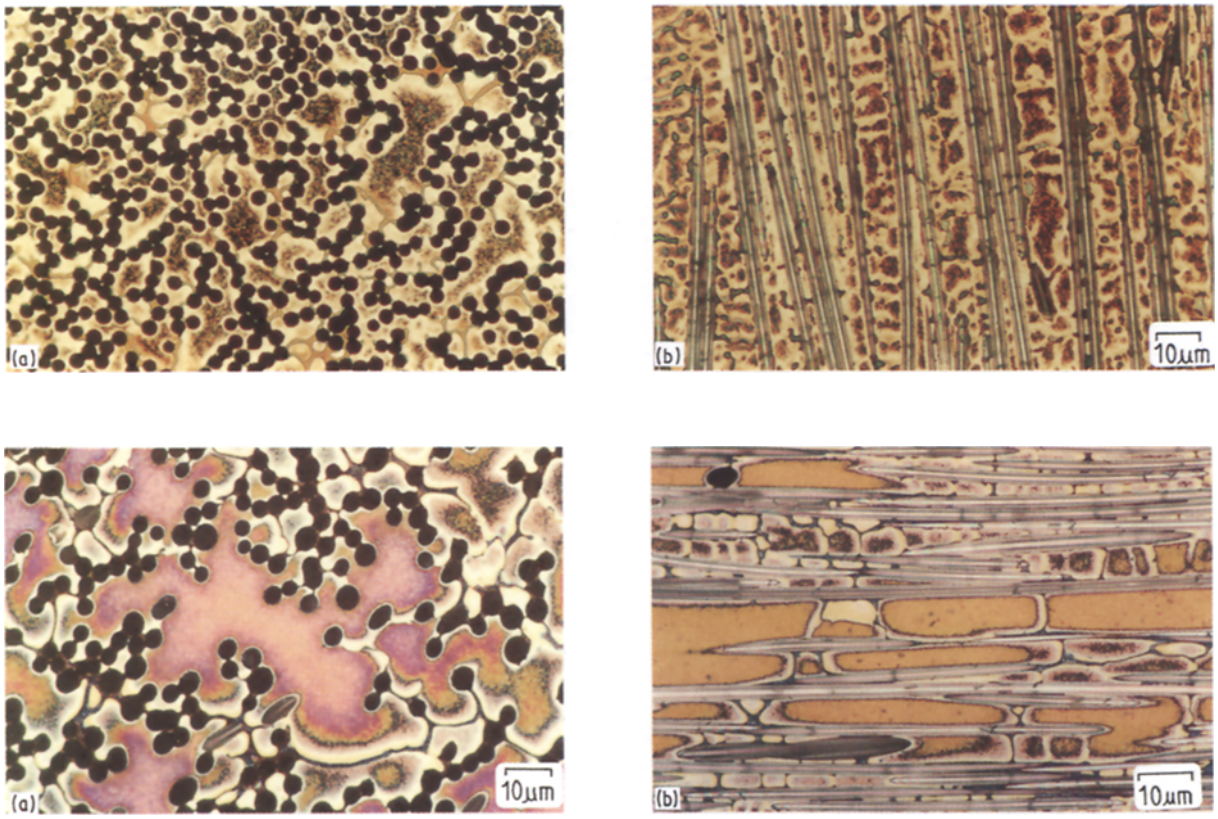

Figure 7 Optical micrographs taken from sample 2 with a local solidification time of 30 s, (a) is transverse and (b) parallel to the fibre direction.

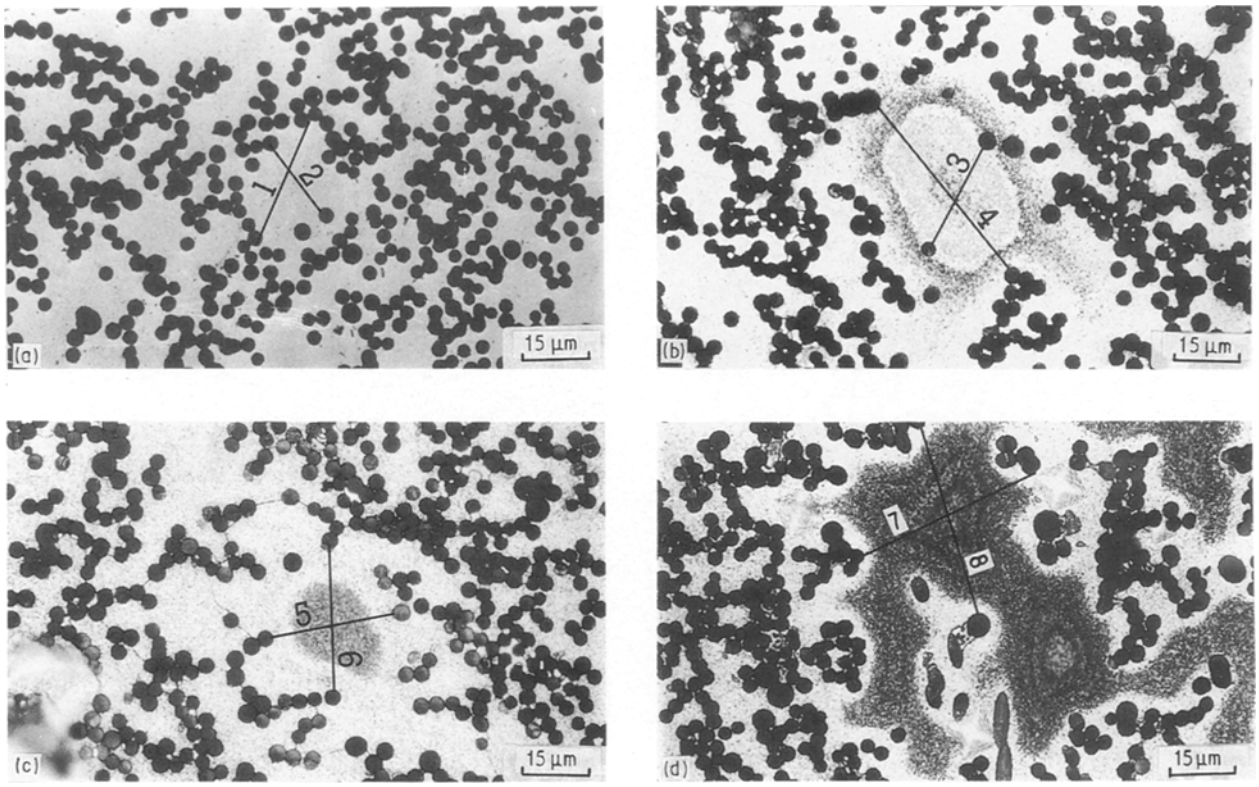

Figure 6 Optical micrographs of etched sections transverse to the fibre direction showing the lines along which microprobe analyses were performed for sample 7, (a); sample 8, (b); sample 9, (c); and sample 10, (d).

TABLE III Matrix copper concentrations measured by EPMA along the lines shown in Fig. 6 using steps of 5 μm. Compositions in wt % Cu

Sample	θ_t (s)	Line	Distance along line (μm)						
			0	5	10	15	20	25	30
7	520	1	5.4	4.9	4.6	4.6	4.8	5.1	5.3
		2	5.4	4.9	4.6	4.8	5.0	5.2	–
8	286	3	3.6	3.2	2.7	2.6	2.7	3.0	–
		4	3.1	2.9	2.8	2.6	2.6	2.8	3.6
9	186	5	2.8	2.4	2.2	2.3	2.9	–	–
		6	2.7	1.9	2.0	2.5	3.1	3.6	
10	110	7	2.9	2.8	2.2	2.1	2.1	2.6	3.2
		8	3.7	2.5	1.9	1.8	2.0	2.4	3.2

3.2. Interrupted solidification experiments

The results of these experiments are summarized in Table I, with all samples being cooled under identical conditions prior to quenching from the semi-solid state. A transverse section, taken from sample number 2, is shown in Fig. 7a. It is evident from the etching effects that, at this early stage of freezing, there were significant variations in copper content within the matrix, although some of this was probably an artefact of quenching. Clearly the solid α-Al did not nucleate preferentially on the fibres, but instead started to grow in interfibre regions, and was growing towards the fibres at the time of the quench. The α-Al does not appear to have readily incorporated the Al_2O_3 fibres during growth but the growth pattern indicates that it grew around the fibres, and where possible in between fibres. Where fibres were very close together, however, the growing α appears to have been unable to develop a sufficiently small radius to grow between them. The longitudinal section from the same sample, Fig. 7b, shows that "secondary dendrite arms", or at least longitudinal perturbations, did indeed form at this early stage of growth, and that they were elongated parallel to the fibre direction. These growth perturbations were only visible in the longitudinal sections of samples 1 to 3. In samples 4 and 5 it was not possible to distinguish such growth forms with residual liquid channels between them, although microsegregation patterns were still evident. In samples 6 and 7 there was virtually no remaining evidence of their existence. It thus appeared that coarsening and coalescence of "secondary arms" occurred exceedingly rapidly with very rapid elimination of residual, solute-rich, liquid channels between "arms". The removal of periodic compositional variations in the direction parallel to the fibre axis was, however, somewhat less rapid. In

longitudinal sections "secondary arms" thus disappeared after a local solidification time of about 100 s, but longitudinal microsegregation persisted until t_f reached about 300 s.

With regard to the transverse section of Fig. 7a it is apparent that the fibre distribution is not uniform and probably not random. As in Figs 3a to 5a there is evidence for chaining and clustering of fibres. Fibres will interfere with the growth of the α in two ways. Firstly they will act as barriers to solute diffusion leading to a pile-up of solute atoms in the liquid between growing α and a fibre. Secondly, because of their much lower thermal conductivity than α-Al, they will influence the heat flow around the growing α. The interaction between growing solid and ceramic fibres or particulate is a complex one. It is not clear, from the present study, whether the fibres were being pushed ahead of the growing solid or whether they were sufficiently rigid to resist movement. It is, however, important to realise that these small diameter, aligned Safimax fibres may well behave very differently from either aligned fibres of much larger diameter or a preform of cross-linked chopped fibres such as Saffil [13].

Microsegregation in these interrupted solidification samples was measured, as before, using EPMA. Suitable areas, typically 15 to 25 μm across, were identified on transverse sections, and point analyses performed at 5 μm intervals along lines in the α-Al matrix. Fig. 8a and b show lines along which analyses were made in samples 1 and 5. Several similar line scans were carried out on each sample listed in Table I and typical results are listed in Table IV. It is apparent that under the cooling conditions employed (total solidification time of each quenched sample would have been $\simeq$ 520 s) the composition within the matrix, away from the fibres, was always relatively uniform. The initial minimum solid composition of approximately 1.2 wt % Cu is consistent with a relatively small growth undercooling for an alloy of bulk composition (C_0) 6 wt % ($kC_0 \simeq$ 1.1 wt % for this alloy). As the time spent in the semi-solid state increased, then the minimum matrix composition increased significantly. This was particularly evident in samples 6 and 7 which were both quenched from below 600 °C, at which temperatures the residual liquid would have been extremely solute rich. Sample 6 had a minimum solute level of 2.3 wt % and in sample 7 it was 4.6 wt %. In this latter sample some matrix compositions were near the maximum solid solubility of Cu in Al of 5.6 wt %. This of course implies that the fraction of eutectic at the end of freezing must have been small and the limited amount of $CuAl_2$ evident in Fig. 3a and b qualitatively supports this.

It is evident from the micrographs of Figs 7 and 8 that the α-Al grew such that pools of solute-rich liquid became trapped around fibres; the average spacing of these pools being of the same order as the average interfibre spacing, λ_f ($\lambda_f \simeq 6$ μm). It is well known that in the latter stages of freezing steep solid composition gradients develop at the solid–liquid interface and back-diffusion of solute into the solid can become an important effect [1].

It seems probable, therefore, that the increase in matrix composition which occurred towards the end of freezing was caused by such back-diffusion from melt puddles with a spacing of the order of λ_f. This situation is quite different from that of an unreinforced alloy where the solute-rich liquid pools have a spacing of the order of λ_s which in an unreinforced alloy is $\simeq$ 65 μm.

4. Further discussion and analysis

4.1. Microstructural development

The present observations indicate clearly that closely spaced fibres inhibit the development of crystallographically oriented dendritic structures. It is clear that as suggested by Mortensen *et al.*, [16] fibres have a major effect when $\lambda_f/\lambda_s < 1$ where λ_s is the secondary dendrite arm spacing in an unreinforced alloy having the same total freezing time. The interrupted solidification samples were furnace cooled in such a way that the temperature gradients in the sample were virtually zero. These are conditions which give equiaxed dendritic growth in an unreinforced alloy [10], but gave non-dendritic growth in the composite. It is possible to gain further insight into the reasons for this by considering the Kurz and Fisher model for dendritic growth [5]. Assuming the temperature gradient, G, to be zero it is possible to calculate the relationship between dendrite tip radius and dendrite tip undercooling. This has been done for three different alloy compositions as shown in Fig. 9 (physical parameters used in the calculation are listed in Table V). From the experimentally recorded temperature against time traces of the interrupted solidification experiment, the maximum growth undercooling at the point of recalescence was $\simeq$ 2 K. Fig. 9 thus predicts a dendrite tip radius of 3 to 4 μm. It is

TABLE IV Matrix copper concentrations measured by EPMA in interrupted solidification samples. Typical lines are shown in Figs 6 and 8 and analysis points were separated by 5 μm. Compositions in wt % Cu

Sample	t_f (s)	Line	Fig.	Distance along line (μm)					
				0	5	10	15	20	25
1	18	9	8	1.2	1.2	1.2	1.2	1.2	1.2
2	30			1.5	1.2	1.2	1.0	1.2	1.2
3	90			1.6	1.5	1.4	1.6	1.6	1.5
4	160			2.0	1.7	1.6	1.6	1.6	1.7
5	220	10	8	2.4	2.4	2.1	2.1	2.1	2.2
6	310			2.7	2.4	2.3	2.6	2.7	3.4
7	520	2	6	5.4	4.9	4.6	4.6	4.8	5.1

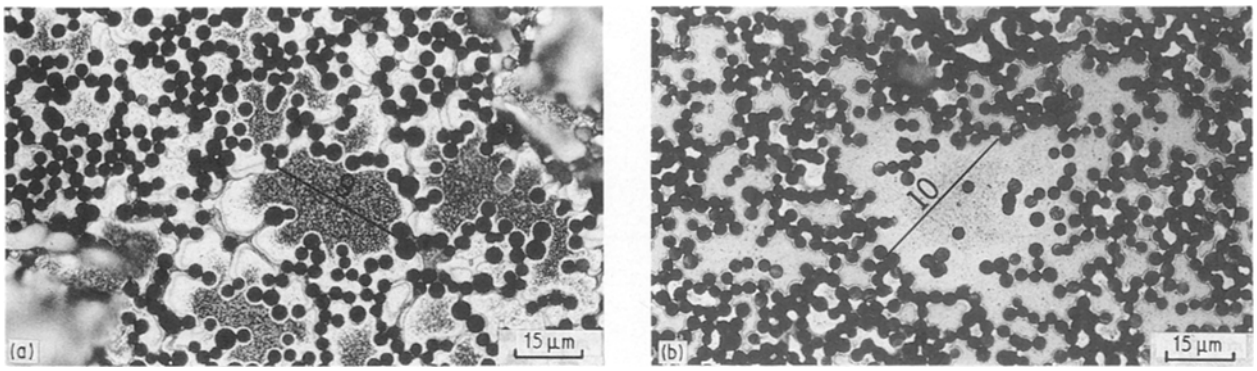

Figure 8 Etched sections transverse to the fibre direction showing lines along which microprobe analyses were performed for the interrupted solidification samples, 1, (a) and 5, (b).

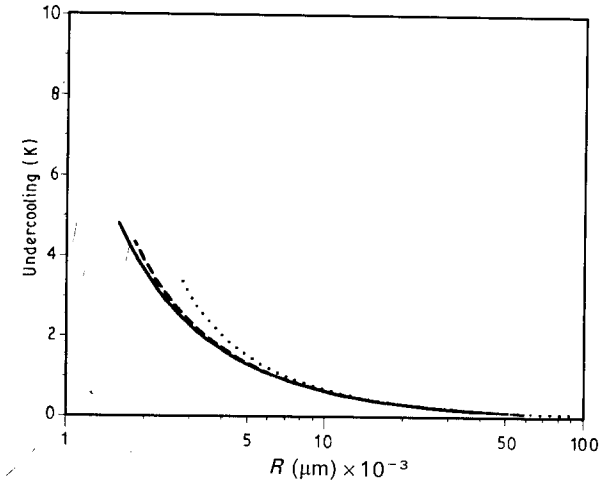

Figure 9 Plot of dendrite tip undercooling against tip radius, R, for Al–Cu alloys of three different compositions using the model of reference [5]. (· · · · ·) 2 wt % Cu, (– – –) 4.5 wt % and (——) 6 wt %.

TABLE V Physical parameters used in the calculations

Parameter	Value
D_l [1]	3×10^{-3} mm^2 s^{-1}
k [9]	0.18
θ [23]	2.4×10^{-4} K mm
m [1]	-2.6 K wt %$^{-1}$
D_s [9]	4.6×10^{-7} mm^2 s^{-1}

D_l is the solute diffusivity in the liquid, m the liquids slope, k the partition coefficient and θ the curvature under cooling constant.

known [2] that the initial secondary dendrite arm spacing in an alloy is approximately 2.2 times the tip radius, and so in the samples 1 to 7 an initial secondary arm spacing of around 9 μm would be predicted. This indicates that, even for a dendrite tip advancing parallel to the fibre direction, stable dendritic growth with normal sidebranching will be severely inhibited by the fibres in these samples (since $\lambda_f \simeq 6$ μm) as is indeed observed. Sekhar and Trivedi [19] have recently reported this effect in a transparent organic material solidified in a narrow channel. The present observations are also in agreement with earlier studies of Mortensen *et al.* [18] who found that dendritic structures in Al–4.5 wt % Cu began to degenerate in narrow channels, although these were somewhat larger than the interfibre spacing of the present study. Also both these sets of experiments were performed on unidirectionally solidified samples in which dendrites were, in general, forced to grow with ⟨1 0 0⟩ parallel to the channel axis.

In the present non-unidirectional solidification situation, it is possible that initial growth will occur preferentially parallel to the fibre axis in fibre-free channels but along a direction which is not a ⟨1 0 0⟩ type. Sekhar and Trivedi [19] observed this, and found that a complex branching pattern developed. The initial growth perturbations seen, for example, in Fig. 7b from sample 2 ($t_f = 30$ s) were therefore probably formed in a similar way.

These initial growth perturbations were found to be absent in the final structure for θ_t values in excess of about 10 s. Only sample 1, with $\theta_t \simeq 1$ s, exhibited well defined growth perturbations after freezing was complete as seen in Fig. 5b. The interrupted solidification experiments showed that under freezing conditions with $\theta_t = 520$ s the growth perturbations disappeared at $t_f \simeq 100$ s by a mechanism involving coarsening and coalescence. Mortensen *et al.* [18] also observed the disappearance of secondary dendrite arms (similar to the growth perturbations in the present study) and developed a mathematical model for the process. They calculated that for $\theta_t = 520$ s, secondary arms disappear after $t_f = 110$ s, and that θ_t must be less than about 2 s for secondary dendrite arms to appear in the final structure. The present situation is much more complex than either their experimental or model geometries. It is, therefore, perhaps fortuitous that their calculated times, for a channel of diameter 18 μm, are close to those observed experimentally in this work. It is encouraging to note, however, that their experimental results were not dissimilar to those in this work. They found, for example, that when $\theta_t = 417$ s there were no dendrite sidearms in a channel of diameter $\simeq 18$ μm when t_f exceeded about 100 s.

4.2. Microsegregation

The present observations on microsegregation can be compared with previous EPMA measurements by Mortensen and co-workers [15, 18] who found, in fibre-reinforced alloys, reduced microsegregation similar to that reported here; albeit with much larger diameter fibres than those used presently. Hunt and

McCartney [24], and Mortensen *et al.* [18] have both modelled cellular–dendritic solidification in narrow channels and examined the effect of channel diameter on microsegregation in the solid phase. They have employed quite different methods, but have demonstrated that reduced compositional variations and increased minimum solute levels are to be expected when the solid phase grows in narrow channels because of the significant effect of solid state diffusion whilst freezing is taking place. This is often termed back-diffusion [1] and qualitatively explains the measurements in Tables III and IV.

The present geometrical arrangement of fibres is much more complex than the channels assumed in the mathematical models [18, 24]. Nevertheless, a semi-quantitative analysis of the degree of microsegregation in the present work can be obtained by using the Clyne–Kurz modification [25] of the Brody–Flemings [26] microsegregation model which incorporates back-diffusion of solute in the solid. Composition profiles cannot be predicted using such a model, only the fraction of eutectic in the final solidified sample. This parameter is, however, obviously a measure of the degree of homogenization. Using the Clyne–Kurz model the eutectic fraction, f_e, is given by

$$f_e = 1 - \left(\frac{1}{1 - 2\Omega k}\right)\left[1 - \left(\frac{C_e}{C_o}\right)^{(1-2k)/(k-1)}\right] \quad (1)$$

$$\Omega = \left\{\alpha\left[1 - \exp\left(-\frac{1}{\alpha}\right) - 0.5\exp\left(-\frac{1}{2\alpha}\right)\right]\right\} \quad (2)$$

$$\alpha = \frac{4D_s\theta_t}{L^2} \quad (3)$$

where C_e is the eutectic composition (wt %), C_o the alloy composition (wt %), D_s the solute diffusivity in the solid ($mm^2\,s^{-1}$), k distribution coefficient (dimensionless), L the average length of a solidification volume element, α diffusion parameter (dimensionless) and Ω the modified diffusion parameter (dimensionless). Using the data given in Table V, f_e was calculated as a function of α for different alloy compositions as shown in Fig. 10. It is clear from the experimental observations presented in this paper that the last regions of solute-rich liquid to solidify are located around the fibres. The value of the parameter L in Equation 3 can thus, as a first approximation, be set equal to λ_f. Using the value of D_s given in Table V and taking $\lambda_f = 6$ μm then $\alpha = 0.05$ when $\theta_t = 1$ s and when $\theta_t = 520$ s, $\alpha = 26.6$, thus from Fig. 10 it is clear that f_e values are predicted to be 0.12 and 0.02, respectively, for the above values of α. In other words this simple analysis including back diffusion predicts that when $\theta_t = 520$ s freezing conditions give almost the equilibrium eutectic fraction whereas when $\theta_t = 1$ s the amount of eutectic is close to that for non-equilibrium freezing as given by the Scheil equation [1]. From mass balance considerations the matrix must contain a greater fraction of solute if f_e is reduced below the Scheil equation value and, as is shown elsewhere [18, 24, 26], back-diffusion reduces compositional variations within the matrix and increases the minimum matrix composition, thus the observation of a virtually homogeneous matrix when $\theta_t = 520$ s is exactly what is predicted by this simple analysis. Moreover, the changes in segregation profile with decreasing θ_t also accord with the decreasing homogeneity of the matrix predicted by the model.

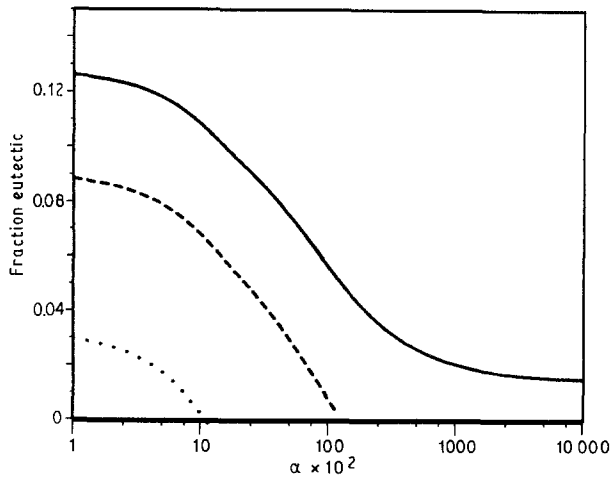

Figure 10 Plot of fraction eutectic against α for Al–Cu alloys of three different compositions using Equations 1 to 3, and data from Table V. (·····2 wt % Cu, – – –4.5 wt % Cu, ——6 wt % Cu).

As noted earlier the EPMA of interrupted solidification samples showed (i) that the initial dendrite growth undercooling was relatively small – similar to that in an unreinforced alloy – and (ii) that minimum matrix compositions increased rapidly in the latter stages of freezing. These observations are broadly in agreement with the work of Mortensen *et al.* [18] and Gungor [27] on systems with larger diameter fibres. It is apparent though that in the present system, with a smaller value of λ_f, higher values of minimum matrix composition and more extensive homogenization occur at much shorter total freezing times. This is indeed exactly what would be predicted from Fig. 10 since α is proportional to $(\theta_t\lambda_f^{-2})$.

Furthermore the predictions of Fig. 10 for an Al–2 wt % Cu alloy are important from the point of view of mechanical properties. It has been shown [28] that a brittle phase at the fibre–matrix interface can adversely affect fracture strength. An Al–2 wt % Cu alloy is, however, predicted to contain no eutectic for $\theta_t > 3$ s, and this effect should be borne in mind when selecting matrix alloys to obtain optimum mechanical properties.

5. Summary and conclusions

The influence of 30 vol %, 3 μm diameter, aligned alumina fibres on the solidification behaviour of an Al–6 wt % Cu alloy has been studied. Composite bars were prepared using a conventional squeeze infiltration process and samples cut from these were subjected to remelting and resolidification under a range of different conditions. The total solidification time, θ_t, was varied from 520 to 1 s, and interrupted solidification experiments were also performed to study

microstructural development as a function of local solidification time, t_f.

Interrupted solidification experiments have been used to study the development of microstructure and microsegregation. It has been found that the α-Al begins to grow within interfibre regions, and grows towards the Al_2O_3 fibres, avoiding them were possible. Consequently fibres are located in the liquid pools which are last to solidify. Growth perturbations, similar to dendrite side-arms, have been found to develop in the early stages of freezing, but these disappear by coarsening and coalescence. Their rate of disappearance is much more rapid than in fibre free alloys and hence they may not be observable in the final solidified structure.

EPMA of the interrupted solidification samples has shown that the initial dendrite composition is not dissimilar to that of an unreinforced alloy, but that the minimum matrix composition increases rapidly in the latter stages of freezing; presumably by back diffusion of solute.

The matrix microstructure and microsegregation have been found to vary significantly with θ_t. The final solidified microstructure is non-dendritic when the ratio λ_f/λ_s falls below 1, to a first approximation. When this occurs the last liquid to solidify is located predominantly around the fibres giving a layer of $CuAl_2$ at the fibre–matrix interface. In the present system such a microstructure has been found to develop when $\theta_t > 10$ s. When θ_t is approximately 1 s it has, however, been found that the final microstructure is dendritic and the $CuAl_2$ more dispersed.

EPMA measurements have shown that the minimum matrix composition increases with increasing θ_t, and that this is accompanied by an increasing homogeneity of the matrix. Minimum matrix compositions of approximately 5 wt % Cu have been obtained for $\theta_t = 520$ s. These compositional variations have been explained in terms of a simple analytical model, incorporating back-diffusion of solute in the solid α-Al phase, in which the average spacing of the liquid pools which are last to solidify is set equal to λ_f.

References

1. W. KURZ and D. J. FISHER, "Fundamentals of Solidification" (Trans Tech, Aedermansdorf, 1986) pp. 65–96.
2. R. TRIVEDI and K. SOMBOONSUK, *Mater. Sci. Engng* **65** (1984) 65.
3. M. C. FLEMINGS, "Solidification Processing" (McGraw-Hill, New York, 1974) p. 150.
4. K. P. YOUNG and D. H. KIRKWOOD, *Met. Trans.* **A6** (1975) 197.
5. W. KURZ and D. J. FISHER, *Acta Metall.* **29** (1981) 11.
6. J. D. HUNT, in Proceedings Conference on Solidification and Casting of Metals, Sheffield, July 1977 (Metals Society, London, 1979) p. 3.
7. M. RAPPAZ and PH. THÉVOZ, *Acta Metall.* **35** (1987) 1487.
8. *Idem., ibid.* **35** (1987) 2929.
9. D. H. KIRKWOOD, *Mat. Sci. Engng* **65** (1984) 101.
10. T. F. BOWER, H. D. BRODY and M. C. FLEMINGS, *Trans. AIME* **236** (1966) 624.
11. M. H. BURDEN and J. D. HUNT, *J. Cryst. Growth* **22** (1974) 99.
12. P. N. QUESTED and M. McLEAN, *Mater. Sci. Engng* **65** (1984) 171.
13. T. W. CLYNE and J. F. MASON, *Met. Trans.* **18A** (1987) 1519.
14. C. R. COOK, D. I. YUN, and W. H. HUNT Jr., in "Cast Reinforced Metal Composites" (American Society of Metals, Metals Park, Ohio, 1988) p. 195.
15. J. A. CORNIE, A. MORTENSEN, M. N. GUNGOR and M. C. FLEMINGS, in Proceedings of the 5th International Conference on Composite Materials, edited by W. C. Harrigan, J. Strife and A. K. Dhingra (TMS, Warrendale, 1986) 809.
16. A. MORTENSEN, M. N. GUNGOR, J. A. CORNIE and M. C. FLEMINGS, *J. Met.* **38** (1986) 30.
17. J. A. CORNIE, A. MORTENSEN and M. C. FLEMINGS, in Proceedings of the 6th International Conference on Composite Materials, edited by F. L. Matthews, N. C. R. Buskell, J. M. Hodginson, and J. Morton (Elsevier Applied Science, London, 1987) p. 2.297.
18. A. MORTENSEN, J. A. CORNIE and M. C. FLEMINGS, *Met. Trans.* **19A** (1988) 133.
19. J. A. SEKHAR and R. TRIVEDI, *Mater. Sci. Engng* **A114** (1989) 133.
20. G. R. CAPPELMAN, J. F. WATTS and T. W. CLYNE, *J. Mater. Sci.* **20** (1985) 2159.
21. Data Sheet on Safimax (ICI Chemical and Polymers Group, Runcorn, UK, 1987).
22. R. T. DE HOFF and F. N. RHINES, "Quantitative Microscopy" (McGraw-Hill, New York, 1968) p. 283.
23. M. GÜNDÜZ and J. D. HUNT, *Acta Metall.* **33** (1985) 1651.
24. J. D. HUNT and D. G. McCARTNEY, *ibid.* **35** (1987) 89.
25. T. W. CLYNE and W. KURZ, *Met. Trans.* **12A** (1981) 965.
26. H. D. BRODY and M. C. FLEMINGS, *Trans. AIME* **236** (1966) 615.
27. M. N. GUNGOR, PhD Thesis, Massachusetts Institute of Technology (1986).
28. R. TRUMPER and V. SCOTT, in Proceedings of the 3rd European Conference on Composite Materials, edited by A. R. Bunsell, P. Lamicq and A. Masiah (Elsevier Applied Science, London, 1989) p. 139.

Received 17 May
and accepted 26 June 1990